

Global Pathway Analysis of Plasma Assisted Ammonia Combustion

Praise Noah Johnson*, Taaresh Sanjeev Taneja[†] and Suo Yang[‡]

Department of Mechanical Engineering, University of Minnesota – Twin Cities, Minneapolis, MN 55455, USA

Global Pathway Selection/Analysis (GPSA) algorithm helps in analyzing the chemical kinetics of complex combustion systems by identifying important global reaction pathways that connects a source and a sink species. The present work aims to extend the application of GPSA to plasma assisted combustion systems in order to identify the dominant global pathways that govern the plasma and combustion kinetics at various conditions. The reaction cycles involving the excitation of nitrogen to its vibrational and electronic states and the subsequent de-excitation to its ground state are found to control the reactivity of plasma assisted systems. Provisions are made in the GPSA algorithm to capture the dominant reaction pathways and cycles of plasma assisted combustion (i.e., p-GPSA). Further, the analysis of plasma assisted ammonia combustion are presented as an example, which includes the results obtained using both the traditional path flux analysis and p-GPSA. The dominant pathways for the plasma assisted combustion of ammonia are identified along with the dominant excitation—de-excitation loops and their importance are ascertained and verified using path flux analysis.

I. Nomenclature

 $A_{e,i \to i}$ = element flux of the eth element from the ith species to the jth species

 $a_{e,r,i\rightarrow j}$ = elemental flux of the eth element going from the ith species to jth species in the rth reaction

 $C_{e,r,i\rightarrow i}$ = number of the e^{th} atoms transferred from the i^{th} to the j^{th} species in the r^{th} reaction

 $\dot{\omega}_r$ = net reaction rate of the \mathbf{r}^{th} reaction

 $n_{e,r,i}$ = number of e^{th} element going out from i^{th} species in the r^{th} reaction

 $v_{r,i}$ = stoichiometric coefficient of the ith species in the rth reaction $D_{GP,e}$ = dominancy of a global pathway involving the eth element $N_{e,i}$ = number of the eth atoms in a molecule of the ith species

 n_i = number of moles of the i^{th} species

II. Introduction

Offiame stabilization, and emission characteristics of combustion systems [1–5]. Plasma, being composed of charged particles (electrons and ions), can catalyze the production of reactive species (radicals, ions, and excited species) in the combustion system, thereby enhancing the reactivity and heat release. The kinetics of plasma assisted combustion (PAC) involve many new reaction pathways that aid in the production of atomic species (such as *O* atoms) due to the electron impact reactions and the subsequent quenching and relaxation reactions. The improved production of radicals due to PAC kinetics promote faster ignition, reduce emissions, and enhance flame stability [6]. The reaction types specific to PAC consist of electron impact ionization, excitation, dissociative excitation, dissociative ionization, dissociation, de-excitation, attachment, and recombination reactions [6]. The inclusion of these reactions, whose rates depend on the reduced electric field (E/N) and cross sections of the colliding species, brings in additional complexity to the previously intricate combustion chemical mechanisms.

To understand the kinetics of PAC, it is necessary to analyze the consumption of fuel species and production of reactive radicals based on PAC kinetic mechanisms. Several methods exist in the literature [7–11] to identify the

^{*}Ph.D. Student, Student Member AIAA

[†]Ph.D. Candidate, Student Member AIAA.

[‡]Richard & Barbara Nelson Assistant Professor, suo-yang@umn.edu (Corresponding Author), Senior Member AIAA.

aggregate behavior of the oxidation of fuel using the detailed combustion chemistry. One such approach is the Global Pathway Selection (GPS) algorithm, which identifies the important global pathways (GP) connecting a source species and a sink species [11]. The GP's identified using this method can be used to analyze and describe the combustion behavior of the system (i.e., Global Pathway Selection Analysis - GPSA). Several studies demonstrated the ability of GPS to uncover the GP's and delineate the dominant pathways involved in the process [12–14]. Studies also suggested the effectiveness of GPSA as a mechanism reduction tool, based on only retaining the species involved in dominant GP's [11].

One of the recent studies demonstrated the extension of GPSA to include the soot-based kinetics to predict the GP's involving the production of soot (i.e., fuel to soot pathways) from the detailed soot kinetics [15]. The GP's were able to reflect the effect of pressure on soot formation correctly. To further extend the use of GPSA, the current study focus on implementing GPSA for the plasma-assisted combustion systems (p-GPSA) to delineate dominant GP's for different PAC regimes. Firstly, the methodology to extend GPSA to PAC systems will be discussed in Section III. Secondly, the results obtained using p-GPSA for the plasma kinetics of ammonia (NH_3) will be presented and compared to conventional path flux diagrams in Section IV. The importance of identifying different loops (simple cycles in the GP's with no repeated vertices) due to excitation of nitrogen (N_2) to its vibrational state and subsequent de-excitation will be discussed.

III. Methodology

A detailed discussion on GPSA can be found in Gao, Yang, and Sun [11]. However, a brief description is presented for the completeness of the present work. The GPSA methodology is based on identifying the elemental fluxes between different species from the simulation results. Based on the calculated elemental fluxes, an element flux graph is constructed for the element of interest (C, H, O, or N), where each node represents a species, and the edges of the graph represent the magnitude of fluxes. The element flux graph contains an initial source species and a final sink species. Any species with significant flux crossing into or out of them are termed as hub species. After the generation of flux graphs and identification of the hub species, the shortest chemical pathways (fastest reaction pathways to transfer element flux from source to sink species) are identified from the source to sink through the hub species using the reactions in the chemical kinetic mechanism. These short pathways are referred to as Global Pathways (GP's) which connects the source and sink species through a hub species, and is the chemical pathway that transfers element flux from the initial source species (usually fuel) to the final sink species (product). Figure 1 shows the steps involved in the analysis using the GPSA algorithm.

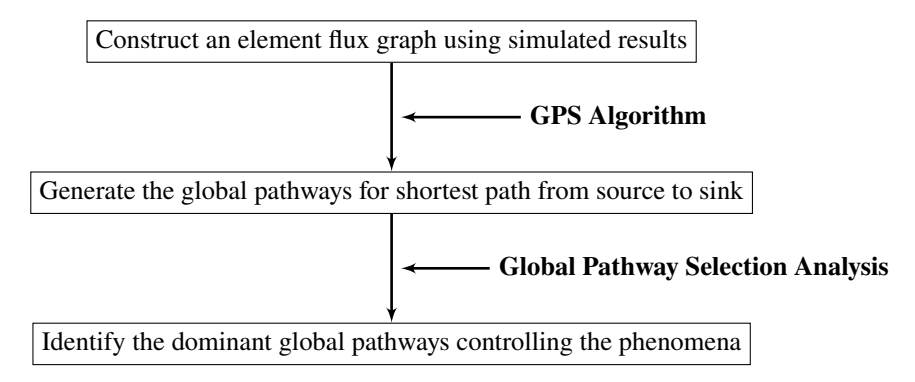


Fig. 1 Various steps involved in performing global pathway selection analysis (GPSA).

A. Identification of Hub Species

The first step in the GPSA framework involves the generation of an element flux graph, where each node represents a species, and the arrows connecting two nodes represent the elemental flux transfer between the two species. The elemental flux of the e^{th} element going from the i^{th} species to the j^{th} species $(A_{e,i\rightarrow j})$ is given by

$$A_{e,i\to j} = \sum_{r} a_{e,r,i\to j} \tag{1}$$

where, $a_{e,r,i\to j}$ represents the elemental flux of the e^{th} element going from the i^{th} species to the j^{th} species for the r^{th} reaction and is given by

$$a_{e,r,i\to j} = \max(0, C_{e,r,i\to j}\dot{\omega}_r) \tag{2}$$

In Eq. 2, $\dot{\omega}_r$ represents the reaction rate of the \mathbf{r}^{th} reaction, whereas, $C_{e,r,i\to j}$ is the elemental flux from \mathbf{i}^{th} species to \mathbf{j}^{th} species through the \mathbf{r}^{th} reaction and is depicted by Eq. 3. Only the positive elemental flux from the \mathbf{i}^{th} species to the \mathbf{j}^{th} species is considered in calculation of $a_{e,r,i\to j}$.

$$C_{e,r,i\to j} = \begin{cases} n_{e,r,j} \frac{n_{e,r,i}}{n_{e,r}}, & \text{if } \nu_{r,j} \nu_{r,i} < 1\\ 0, & \text{otherwise} \end{cases}$$
 (3)

In Eq. 3, $n_{e,r,i}$ represents the number of the e^{th} element going out from the i^{th} species in the r^{th} reaction and $n_{e,r,j}$ represents the number of the e^{th} element going to the j^{th} species in the r^{th} reaction. A negative $v_{r,j}v_{r,i}$ denotes the presence of the i^{th} and j^{th} species at the opposite ends of a reaction, thereby enabling a transfer of the e^{th} element from the i^{th} to j^{th} species in that particular reaction.

Now that the element flux graph is developed using all species in the chemical kinetic mechanism, the global pathways from the source to sink can be obtained by introducing the 'hub species'. A species is selected as the hub species when the normalized element flux going out or coming into the species is greater than a specified threshold (α_{crit}). As the threshold increases, the number of hub species also increases. Eq. 4 defines the threshold criteria to identify the hub species.

$$\frac{\max\left(\sum_{k} a_{e,i\to k}, \sum_{k} a_{e,k\to i}\right)}{\max_{M} \left[\max\left(\sum_{k} a_{e,M\to k}, \sum_{k} a_{e,k\to M}\right)\right]} \equiv \alpha_{e,i} \ge \alpha_{crit} \tag{4}$$

B. Identification of Global Pathways

The global pathways (GP's) connecting the source and sink through each hub species is obtained by identifying the shortest (fastest) chemical reaction pathways to transfer atoms from the source to sink species through hub species. Every identified hub species can have global pathways with the hub species being an integral part of the pathway. The procedure of obtaining the shortest pathways for all hub species has been explained elsewhere in Gao, Yang, and Sun [11].

To understand the behavior of the system, it is necessary to find the dominant pathways governing the kinetics of the system. In order to rank the pathways, the factor 'dominance of a GP' ($D_{GP,e}$) is defined for each global path. The dominance of GP's are calculated as

$$D_{GP,e} = D_{source,e} D_{GP/source,e} \tag{5}$$

where $D_{GP,e}$ represents the fraction (value between 0 and 1) of the e^{th} element that gets transferred through the GP of interest. $D_{source,e}$ is the ratio of total e-atoms in the source species to the total number of initial e-atoms and is depicted in Eq. 6. $D_{GP/source,e}$ represents the fraction of e-atoms going from the source to sink through this GP and is expressed in Eq. 7.

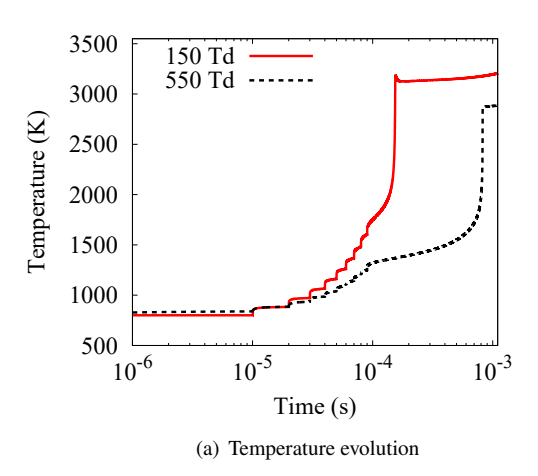
$$D_{source,e} = \frac{n_{source,initial}N_{source,e}}{\sum_{i} n_{i,initial}N_{i,e}}$$
 (6)

$$D_{GP/source,e} = \left(\prod_{i,j \in GP} \frac{A_{e,i \to j}}{\sum_{k} a_{e,i \to k}} \right)^{\frac{1}{|GP|}}$$
 (7)

In Eq. 6, $n_{i,initial}$ represents the initial number of moles of the ith species and $N_{i,e}$ represents the number of the eth atom present in one mole of the ith species. The GP's with the largest values of $D_{source,e}$ are the dominant global pathways. These GP's retain the important chemical information for the configuration of interest and provide insights about the chemistry for the given conditions.

C. Extending GPSA to Plasma Assisted Combustion (PAC)

One of our recent studies [16] explored the PAC of ammonia (NH₃) using our in-house 0D and 1D PAC solvers. The work employed nanosecond pulsed discharges interspersed with microsecond level gaps between pulses. During the nanosecond discharge intervals, the electron impact reactions become predominant owing to their dependence on the strong electric field during discharges. However, during the microsecond gaps, electron-ion recombination,



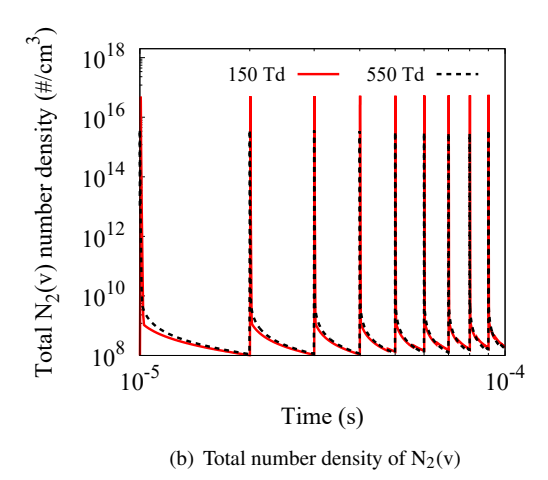


Fig. 2 Temperature and total $N_2(v)$ number density for the 0D plasma assisted combustion of NH_3 /air mixtures at E/N = 150 (red solid line) and 550 Td (black dashed line).

de-excitation, and combustion reactions become more prominent. Thus, during the voltage pulses, both the 1D and 0D solvers, compute the species densities, gas and electron temperatures, and the 1D solver additionally computes the electric field. However, during the microsecond gaps, the solvers only calculates species densities and gas temperature. The details of the 0D and 1D solvers are explained in Taneja & Yang [16] and Yang et al. [17], respectively.

Given the coupling of plasma and combustion kinetics, which enhances the production of key radicals that can accelerate chain branching and propagation, it is important to predict GP's that produce the excited species during the plasma pulse and the GP's that result in quenching of those active species to form the radicals.

The first step in deciding the species and reactions of the plasma mechanism depends on the target mean electron energy range / target reduced electric field (E/N). If this range is much smaller or much larger than the thresholds of certain electron impact reactions, those reactions can safely be removed from the mechanism, as their rate coefficients would be negligible. For instance, for the study of NH₃ combustion in O_2 and He, vibrational excitation reactions of ammonia were excluded as their thresholds were much smaller than the target mean energy range of 5 - 15 eV. Next, the 0D/1D solver can be used to obtain the production / consumption rates of important, but short-lived "plasma species" and their effect on the relatively long-lived "combustion radicals". This basic approach can be used to identify hub species and reactions which kinetically interesting phenomena such as ignition, flame stabilization and emission. Further, the global pathways effected by the plasma reactions could be identified by using the the aforementioned GPSA algorithm. Effect of different variables such as pulse repetition frequency, peak voltage, equivalence ratio, energy density per pulse, ambient temperature, pre-ionization levels, etc. on the kinetics of PAC can be quantified for different fuel / oxidizer combinations using the p-GPSA.

The original GPSA algorithm [11] developed for the analysis of combustion systems identifies the dominant GP's without any cycles (loops involving two species A and B which results in the cycle $A \longrightarrow B \longrightarrow A$). Thus for an analysis of NH₃ combustion using the original GPSA, the cycle produced by the formation of NH₂ radicals by H-abstraction, followed by the reversion of NH₂ radicals to NH₃ by a recombination reaction (NH₃ \longrightarrow NH₂ \longrightarrow NH₃) would not be considered as part of any global pathway. For plasma assisted combustion systems, the excitation of certain species to their electronic and vibrational states followed by their de-excitation to the ground state has significant importance in radical production (O radicals) and the consumption of fuel. However, these reactions form a cycle, which would be discarded by the conventional GPSA.

To further understand the need to identify important loops in plasma kinetics, simulations are performed for the nanosecond pulsed discharge combustion of stoichiometric NH₃/air mixture using our in-house 0D code [16] at different E/N (150 and 550 Td, 1 Td = 10^{-17} V cm²), temperature of 800 K, pulse frequency of 100 kHz, and atmospheric pressures. Figure 2(a) and (b) depicts the simulated results for temperature evolution and the total number density of all vibrational states of nitrogen ($N_2(v1)$, $N_2(v2)$, upto $N_2(v8)$), respectively. At low E/N (150 Td), NH_3 is found to ignite faster ($\sim 1 \times 10^{-4}$ s, see Fig. 2(a)). This increased reactivity at 150 Td could be attributed to the higher rate of rise in temperature during each pulse. A conventional path flux analysis is performed to ascertain the higher rise in temperature at 150 Td and is depicted in Fig. 3. The path flux analysis in Fig. 3 shows the consumption of ammonia

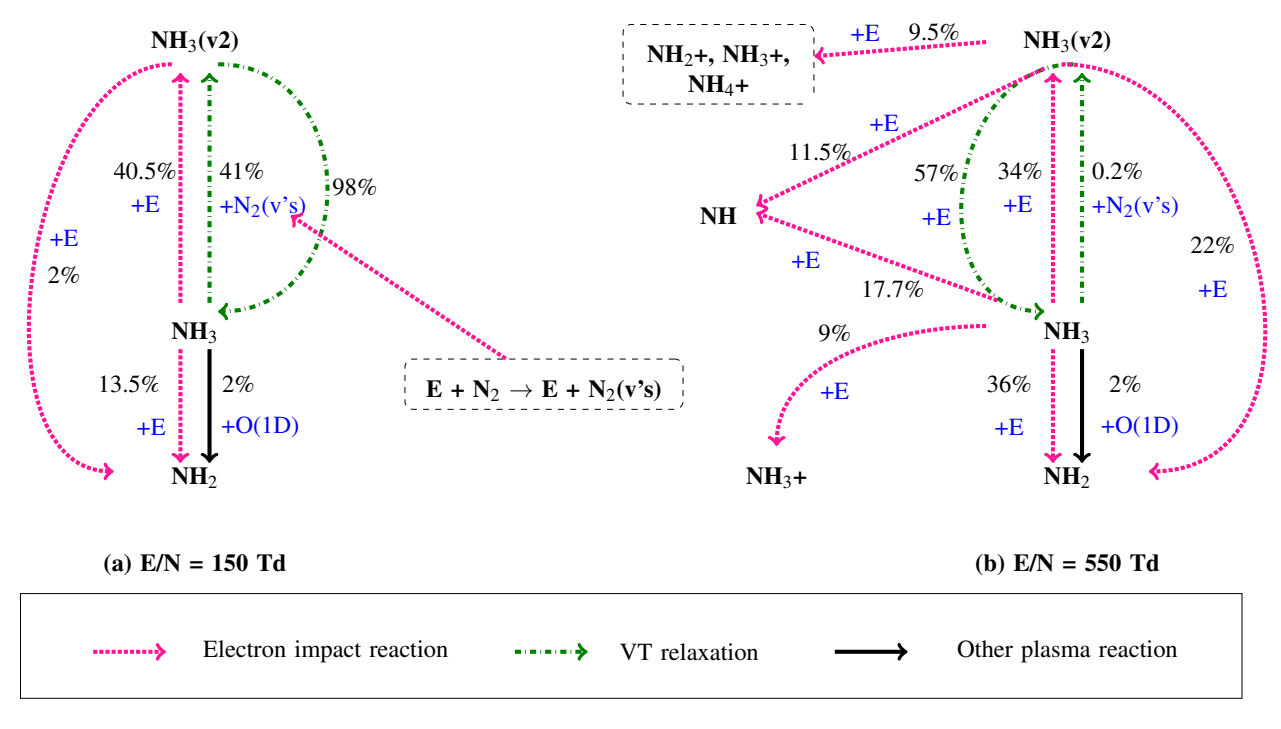


Fig. 3 Conventional path flux analysis for the consumption of NH₃ at a) E/N = 150 Td, and b) 550 Td.

leading to immediate fuel intermediates. At 150 Td, it can be seen that about 41% of NH₃ excites to its vibrational state NH₃(v_2) through the relaxation of N₂(v) by the reaction

$$NH_3 + N_2(v) \longrightarrow NH_3(v_2) + N_2 \tag{R1}$$

This forms a cycle wherein, the $N_2(v)$'s formed by the electron impact reaction $E + N_2 \longrightarrow E + N_2(v)$ proceeds to undergo a vibrational-translational relaxation (VT relaxation given by R1), producing N_2 . Also, Fig. 2(b) shows the large production of $N_2(v)$ during the pulse and their immediate de-excitation at the end of pulse (almost vertical lines). Moreover, all of the $NH_3(v2)$ formed ($\sim 98\%$) relaxes back to its ground state at 150 Td. These cycles release energy to the mixture during the relaxation of the excited species to ground state, causing the temperature to rise resulting in increased reactivity. In comparison, there is no formation of $NH_3(v2)$ through the VT relaxation of $N_2(v)$ species at 550 Td. This explains the lower rate of rise in temperature and lesser reactivity at 550 Td.

Thus, it is essential to capture the cycles formed due to the excitation and de-excitation of species like N_2 , owing to their importance at certain conditions. Based on these observations, the current study considers the inclusion of cycles for the p-GPSA, thereby identifying the global pathways, excitation and de-excitation cycles, and their corresponding dominance.

IV. Results and Discussion

This section presents the computed results of the plasma-assisted combustion of NH_3 along with conventional path flux analysis. The dominant GP's and cycles obtained using p-GPSA are analysed and compared to that of conventional path flux method. All the simulations were performed considering a homogeneous isochoric reactor.

A. Plasma Assisted Combustion of NH₃ at Different Reduced Electric Field (E/N)

Our in-house 0D solver [16] is used to simulate the plasma assisted ignition of stoichiometric NH_3 /air mixture. The mode of plasma discharge considered in this work is repetitive nanosecond pulsed discharges with microsecond gaps after each pulses. The frequency of the pulses are set to 100 kHz for all the NH_3 ignition studies. The 0D solver uses a square wave profile for the reduced electric field, with a pulse duration of 5 - 9 ns. The energy deposited in each pulse has been limited to a constant 0.05 J/cm³. The simulations are performed for an initial temperature of 800 K and

Table 1 Dominant global pathways and cycles for the nanosecond discharge PAC of NH₃ at 150 and 550 Td.

Reduced electric field (Td)	Global pathways/cycles	Dominance
150	Tracked by H atom	
	$NH_3 \to H \to NH_2 \to OH \to H_2O$	0.16
	$NH_3 \rightarrow NH_2 \rightarrow OH \rightarrow H_2O$	0.14
	$NH_3 \rightarrow NH_3(v2) \rightarrow NH_2 \rightarrow OH \rightarrow H_2O$	0.13
	$NH_3 \rightarrow NH_3^+ \rightarrow NH_2 \rightarrow OH \rightarrow H_2O$	0.08
	Tracked by N atom	
	$NH_3 \rightarrow NH_2 \rightarrow NH \rightarrow N \rightarrow N_2$	0.38
	$NH_3 \rightarrow NH_2 \rightarrow NH \rightarrow N_2H_2 \rightarrow NNH \rightarrow N_2$	0.37
	$NH_3 \rightarrow NH_2 \rightarrow NH \rightarrow N_2O \rightarrow NO \rightarrow N_2$	0.28
	$NH_3 \rightarrow NH_2 \rightarrow N_2H_2 \rightarrow NNH \rightarrow N_2$	0.27
	Cycles	
	$NH_3 \rightarrow NH_3(v2) \rightarrow NH_3$	0.53
	$N_2 \to N_2(v1) \to N_2$	0.4
	$N_2 \to N_2(v2) \to N_2$	0.33
	$N_2 \rightarrow N_2(v3) \rightarrow N_2$	0.28
	Tracked by H atom	
550	$NH_3 \rightarrow NH_3(v2) \rightarrow H \rightarrow NH_2 \rightarrow H_2O$	0.2
	$NH_3 \to H \to NH_2 \to H_2O$	0.19
	$NH_3 \rightarrow NH_3(v2) \rightarrow NH_2 \rightarrow H_2O$	0.16
	$NH_3 \rightarrow NH_3(v2) \rightarrow NH_3^+ \rightarrow NH_2 \rightarrow H_2O$	0.16
	Tracked by N atom	
	$NH_3 \rightarrow NH_2 \rightarrow NH \rightarrow N_2$	0.35
	$NH_3 \rightarrow NH_2 \rightarrow NNH \rightarrow N_2$	0.34
	$NH_3 \rightarrow NH_3(v2) \rightarrow NH_2 \rightarrow NH \rightarrow N_2$	0.31
	$NH_3 \rightarrow NH_3(v2) \rightarrow NH_2 \rightarrow NNH \rightarrow N_2$	0.3
	Cycles	
	$NH_3 \rightarrow NH_3(v2) \rightarrow NH_3$	0.13
	$N_2 \to N_2(B) \to N_2$	0.12
	$N_2 \to N_2(\mathbf{C}) \to N_2$	0.12
	$N_2 \to N_2(a') \to N_2$	0.11

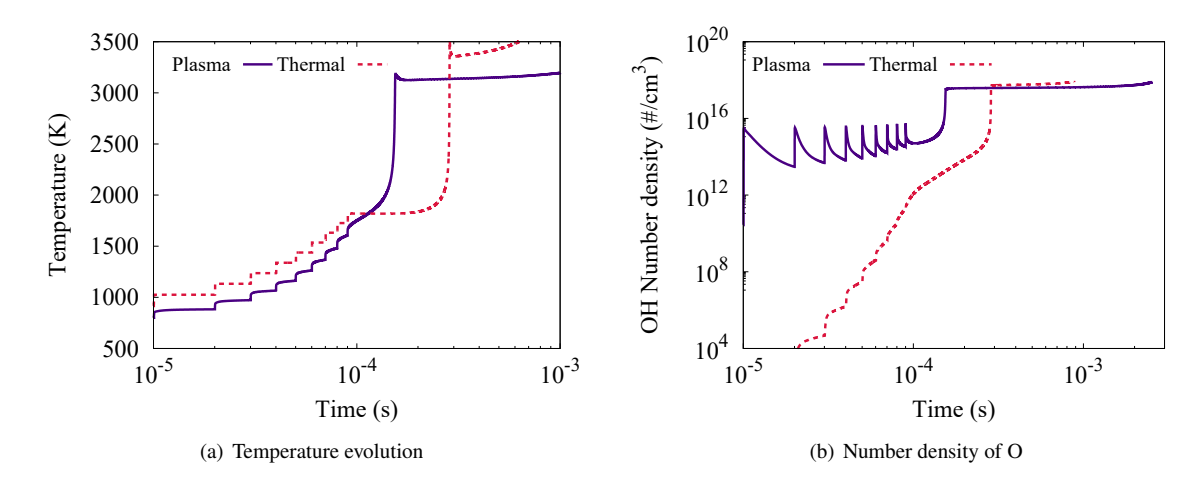


Fig. 4 Temperature and species number density of OH radical for the 0D combustion of NH₃/air mixtures using thermal energy deposition (dashed lines) and plasma energy deposition (solid lines).

atmospheric pressures. The simulated results are then used in the analysis using p-GPSA. Traditional path flux analysis similar to those found in literature [18] are used to compare and validate the analysis done using p-GPSA.

To validate the *p*-GPSA methodology with reference to the observations made in Sec. III, the newly developed tool was used in the analysis of plasma assisted combustion of NH_3 for the conditions specified in Fig. 2. Table 1 represents the dominant GP's and cycles along with their dominance values at reduced electric fields of 150 and 550 Td. The dominant GP's are identified by tracking the element flux transfer of hydrogen (H) and nitrogen (N) atoms with H_2O and N_2 as the sink species respectively. In addition to the GP's, dominant cycles have also been listed for both the cases. At 150 Td, it is observed that the dominant consumption pathway of NH_3 to produce H_2O is $NH_3 \rightarrow H \rightarrow NH_2 \rightarrow OH \rightarrow H_2O$ with a dominance value of 0.16, whereas, at 550 Td, the dominant pathway is found to be $NH_3 \rightarrow NH_3(v2) \rightarrow H \rightarrow NH_2 \rightarrow H_2O$ (dominance = 0.2). This agrees well with the conventional path flux analysis presented in Fig. 3, where, at 150 Td, almost every $NH_3(v2)$ produced relaxes back to NH_3 . This makes the electron impact reaction $NH_3 + E \rightarrow NH_2 + H + E$ the major producer of H radicals and in turn produce H_2O . Moreover, at 550 Td, the dominance of $NH_3(v2)$ in the production of H_2O agrees well with the path flux analysis as 22% of $NH_3(v2)$ proceeds to form NH_2 and another 11.5% produces NH, along with H radicals. Thus the production of H_2O is effected through $NH_3(v2)$ at 550 Td. These observations suggest the consensus between p-GPSA and the conventional path flux diagrams. Similar results can be observed by looking into the GP's identified by tracking elemental flux of N atom.

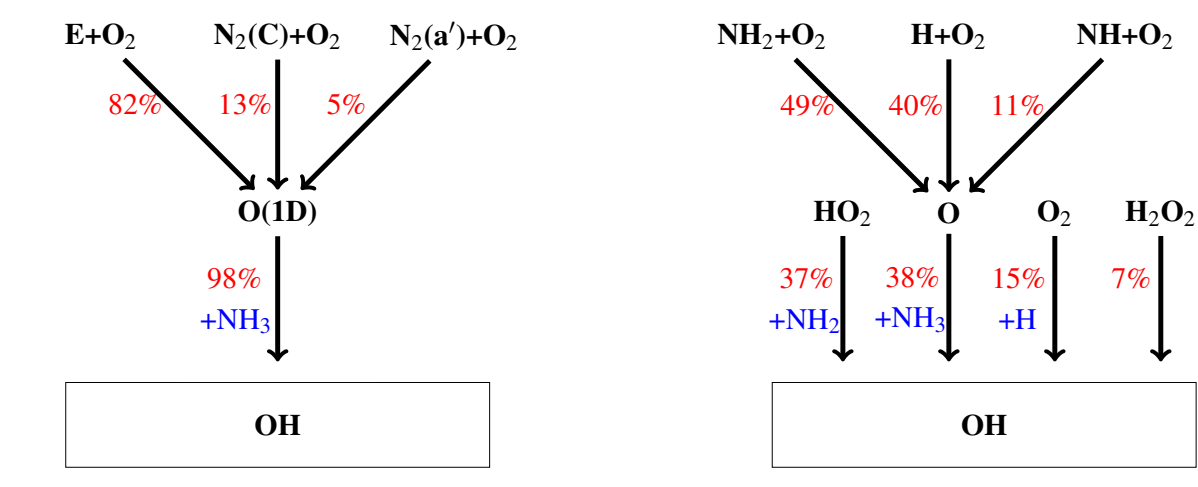
In addition to the GP's identified for the consumption of NH_3 , the dominant cycles involving the excitation and de-excitation of species have been identified using p-GPSA. From Table 1, it can be observed that at 150 Td, the most dominant cycles involve the excitation of NH_3 and N_2 to their vibrational states $(NH_3(v2), N_2(v1), N_2(v2),$ and $N_2(v3)$). In contrast, the vibrational excitation of N_2 are not found to be relevant at 550 Td, as the electronic excitation to $N_2(B)$, $N_2(C)$, and $N_2(a')$ dominates at these condition. These results agree well with the path flux analysis in Fig. 2, where different $N_2(v)$'s are found to play a significant role in the production of $NH_3(v2)$ at 150 Td, whereas, electronic excitation at 550 Td. Thus, extending GPSA for PAC and incorporating the cycles into p-GPSA helps in identifying the important GP's and the dominant cycles which induce heating effects to the system thereby promoting the reactivity.

B. Comparison of Ignition of NH₃ at Different Modes of Energy Deposition

In order to further access the validity of the p-GPSA, simulations are performed for the 0D combustion of stoichiometric NH₃/air mixture with repetitive nanosecond thermal energy depositions. The thermal energy deposited per pulse, frequency of deposition, and number of pulses are set to match the energy deposition at pulsed plasma discharges, so as to compare the nanosecond plasma discharge (at 150 Td) with thermal energy deposition. Figure 4 presents the temperature evolution (Fig. 4(a)) and the number density of OH radical (Fig. 4(b)) of NH_3 air mixture for both plasma (solid lines) and thermal energy deposition (dashed lines). A higher reactivity is observed when the energy deposition occurs through plasma discharges. This could be attributed to the higher production of reactive radicals (like O and OH radical) during the pulses as shown in Fig. 4(b). At the end of the final pulse, the OH number density for

Table 2 Dominant global pathways for the production of OH and cycles for the nanosecond discharge PAC of NH_3 compared to thermal energy deposition.

Mode of energy deposit	Global pathways/cycles	Dominance
	Production of OH radicals	
	$O_2 \to O(^1 D) \to OH$	0.33
Nanagagand plagma	$O_2 \to O(^1 D) \to O \to NO \to OH$	0.2
Nanosecond plasma	$O_2 \to O \to OH$	0.2
	Cycles	
	$N_2 \to N_2(B) \to N_2$	0.2
	$N_2 \to N_2(\mathbf{a}') \to N_2$	0.16
	$N_2 \to N_2(\mathbf{C}) \to N_2$	0.16
	Production of OH radicals	
	$O_2 \to HO_2 \to OH$	0.42
Thermal energy deposition	$O_2 \to HO_2 \to H_2O_2 \to OH$	0.41
Thermal energy deposition	$O_2 \to O \to OH$	0.27



(a) Nanosecond plasma energy deposition

(b) Nanosecond thermal energy deposition

Fig. 5 Path flux analysis for the production of OH radical during a) nanosecond plasma energy deposition, and b) nanosecond thermal energy deposition. All flux percentages are relative to the total production of the respective species.

plasma discharge is found to be four orders of magnitude higher over thermal energy deposition.

To investigate the lower reactivity during the deposition of thermal energy, p-GPSA is used to analyze the global pathways and cycles in the event of thermal energy deposition and is compared to that of the nanosecond plasma discharge. Table 2 portrays the dominant global pathways producing OH radicals (by tracking O atoms) and the corresponding cycles for both plasma and thermal energy deposits. The production of OH radical is chosen for the analysis owing to its high reactivity and its sensitivity to ignition of fuels with hydrogen. From Table 2, dominant global pathway producing OH radical is found to be $O_2 \rightarrow O(^1D) \rightarrow OH$, indicating the significance of the species $O(^1D)$ for the ignition of ammonia. The importance of $O(^1D)$ can also be verified using a conventional path flux diagram provided in Fig. 5(a), where about 98% of OH is been produced by the reaction $NH_3 + O(^1D) \rightarrow NH_2 + OH$. However, for thermal energy deposition, the global pathways and path flux diagram do not contain the species $O(^1D)$, thereby betraying its lower reactivity. Moreover, the p-GPSA identifies the excitation and de-excitation cycles involving

the electronic excitation of nitrogen $(N_2 \to N_2(C) \to N_2)$, which are responsible for the production of $O(^1D)$. No such cycles were found for the case of thermal energy deposition. Thus, the *p*-GPSA is found to be able to capture the global pathways and the cycles responsible for the production of OH radicals for plasma and thermal energy depositions.

These results, along with the analysis of global pathways for the plasma assisted combustion with different E/N further bolsters the ability of p-GPSA in the analysis of 0D plasma kinetics. The ability of p-GPSA to identify important excitation and de-excitation cycles provide an essential tool in the kinetic analysis of plasma assisted combustion.

V. Conclusion and Future Work

The analysis of the dominant global pathways in the combustion system using the Global Pathway Selection and Analysis (GPSA) algorithm has been extended to incorporate the plasma assistant combustion using nanosecond pulsed discharges (*p*-GPSA). The occurrence of different cycles involving the excitation and de-excitation of certain species have been observed, and were found to be critical in the ignition of ammonia. Thus, in addition to the analysis of global pathways, provisions were incorporated in the *p*-GPSA so as to identify the dominant cycles formed by the excitation and relaxation of the excited species. The *p*-GPSA developed in this work was used in the analysis of plasma assisted combustion of ammonia air mixtures at different reduced electric fields (E/N) and was observed to capture the dominant global pathways and cycles dominating the kinetics of ammonia. The results were found to be in accordance with conventional path flux analysis. Further, the *p*-GPSA was used to analyse the difference in the kinetics of ammonia for two different modes of energy deposition: plasma and thermal energy deposition. The results obtained using the present *p*-GPSA and conventional path flux analyses were found to be in good agreement.

The identification of the global pathways and the cycles provide insights into the chemistry of different channels influencing the combustion characteristics of plasma assisted combustion. These insights can be further used to identify the important species and reactions necessary for ignition and can serve as a foundation for the development a mechanism reduction tool to reduce a detailed kinetic model for plasma assisted combustion.

Acknowledgments

S. Yang acknowledges the grant support from NSF CBET 2002635. P.N. Johnson acknowledges the graduate fellowship support from the Department of Mechanical Engineering at University of Minnesota. T.S. Taneja acknowledges the support from the UMII MnDrive Graduate Assistantship Award. The authors acknowledge Prof. Graham V. Candler and the Minnesota Supercomputing Institute (MSI) for the computational resources.

References

- [1] Starikovskiy, A., and Aleksandrov, N., "Plasma-assisted ignition and combustion," *Progress in Energy and Combustion Science*, Vol. 39, No. 1, 2013, pp. 61–110.
- [2] Starikovskaia, S. M., "Plasma assisted ignition and combustion," *Journal of Physics D: Applied Physics*, Vol. 39, No. 16, 2006, p. R265.
- [3] Ombrello, T., Qin, X., Ju, Y., Gutsol, A., Fridman, A., and Carter, C., "Combustion enhancement via stabilized piecewise nonequilibrium gliding arc plasma discharge," *AIAA journal*, Vol. 44, No. 1, 2006, pp. 142–150.
- [4] Lou, G., Bao, A., Nishihara, M., Keshav, S., Utkin, Y. G., Rich, J. W., Lempert, W. R., and Adamovich, I. V., "Ignition of premixed hydrocarbon–air flows by repetitively pulsed, nanosecond pulse duration plasma," *Proceedings of the Combustion Institute*, Vol. 31, No. 2, 2007, pp. 3327–3334.
- [5] Kim, W., Mungal, M. G., and Cappelli, M. A., "The role of in situ reforming in plasma enhanced ultra lean premixed methane/air flames," *Combustion and Flame*, Vol. 157, No. 2, 2010, pp. 374–383.
- [6] Ju, Y., and Sun, W., "Plasma assisted combustion: Dynamics and chemistry," Progress in Energy and Combustion Science, Vol. 48, 2015, pp. 21–83.
- [7] Lam, S., and Goussis, D., "Understanding complex chemical kinetics with computational singular perturbation," *Symposium* (*International*) on *Combustion*, Vol. 22, Elsevier, 1989, pp. 931–941.
- [8] Androulakis, I. P., Grenda, J. M., and Bozzelli, J. W., "Time-integrated pointers for enabling the analysis of detailed reaction mechanisms," *AIChE journal*, Vol. 50, No. 11, 2004, pp. 2956–2970.

- [9] Niemeyer, K. E., Sung, C.-J., and Raju, M. P., "Skeletal mechanism generation for surrogate fuels using directed relation graph with error propagation and sensitivity analysis," *Combustion and flame*, Vol. 157, No. 9, 2010, pp. 1760–1770.
- [10] Sun, W., Chen, Z., Gou, X., and Ju, Y., "A path flux analysis method for the reduction of detailed chemical kinetic mechanisms," *Combustion and Flame*, Vol. 157, No. 7, 2010, pp. 1298–1307.
- [11] Gao, X., Yang, S., and Sun, W., "A global pathway selection algorithm for the reduction of detailed chemical kinetic mechanisms," *Combustion and Flame*, Vol. 167, 2016, pp. 238–247.
- [12] Yang, S., Gao, X., and Sun, W., "Global pathway analysis of the extinction and re-ignition of a turbulent non-premixed flame," 53rd AIAA/SAE/ASEE Joint Propulsion Conference, 2017, p. 4850.
- [13] Gao, X., and Sun, W., "Using Global Pathway Selection Method to Understand Chemical Kinetics," 55th AIAA Aerospace Sciences Meeting, 2017, p. 0836.
- [14] Gao, X., Gou, X., and Sun, W., "Global Pathway Analysis: a hierarchical framework to understand complex chemical kinetics," Combustion Theory and Modelling, Vol. 23, No. 3, 2019, pp. 549–571.
- [15] Zhou, D., and Yang, S., "Soot-based Global Pathway Analysis: Soot formation and evolution at elevated pressures in co-flow diffusion flames," *Combustion and Flame*, Vol. 227, 2021, pp. 255–270.
- [16] Taneja, T. S., and Yang, S., "Numerical Modeling of Plasma Assisted Pyrolysis and Combustion of Ammonia," AIAA Scitech 2021 Forum, 2021, p. 1972.
- [17] Yang, S., Nagaraja, S., Sun, W., and Yang, V., "Multiscale modeling and general theory of non-equilibrium plasma-assisted ignition and combustion," *Journal of Physics D: Applied Physics*, Vol. 50, No. 43, 2017, p. 433001.
- [18] Faingold, G., and Lefkowitz, J. K., "A numerical investigation of NH3/O2/He ignition limits in a non-thermal plasma," *Proceedings of the Combustion Institute*, Vol. 38, No. 4, 2021, pp. 6661–6669.